Journal of Statistical Physics, Vol. 76, Nos. 1/2, 1994

Triangular Dynamics Under Pressure

François Bavaud[1]

Received March 13, 1994

Three planar classical particles interact via a potential proportional to the area of the triangle they form. This system is equivalent to two oscillators attached to the origin, the nearest being repelled by and the other being attracted to it (piecewise integrable Hamiltonian). Numerical simulations show two types of trajectories: those apparently escaping to infinity, and those in confined quasi-periodic orbits. Adiabatic theories lead to discrete recurrence relations and allow for the second type only. A general method allowing prediction of first return time of the slow motion as well as a short/long-period relation is presented. The issue of the possibly metastable nature of escaping trajectories is raised.

KEY WORDS: Pressure ensembles; homogeneous potentials; piecewise integrable Hamiltonians; adiabatic limit; nonlinear discrete dynamics; non-ergodicity; metastability.

1. INTRODUCTION

We consider the following "area" model: three planar classical particles of identical mass are governed by the potential $V(x_1, x_2, x_3) = P\,|K(x_1, x_2, x_3)|$, where $|K|$ is the area of the triangle spanned by the particles and P is the "pressure." Our interest initially stemmed from previous studies of pressure ensembles in statistical mechanics[1]: in this approach, confinement of the n-body system should result from an energetic cost associated with dilute configurations (such that $|K|$ or $|\partial K|$,..., is large), rather than being enclosed in a container Λ as in canonical ensembles.

The corresponding partition function diverges logarithmically, due to "stretched" configurations existing at an arbitrarily low energetic cost: the admissible phase space is unbounded for any positive energy. In this sense, our model shares common features with other "weakly diverging"

Dedicated to Prof. Philippe Choquard.

[1] Institut de Mathématiques appliquées SSP, Université de Lausanne, CH-1015 Lausanne, Switzerland. francois.bavaud@imaa.unil.ch.

0022-4715/94/0700-0645$07.00/0

systems: Carnegie and Percival[2] have investigated the behavior of two one-dimensional particles interacting through some quartic potentials. Simon[3] addressed the issue of whether the quantum analogs of classically "weakly diverging" systems possess a discrete spectrum. The quantum analog of the area model appears to have been investigated by R. Feynman (unpublished) as a "toy model" for quark confinement (Prof. Barry Simon, private communication).

Another salient feature of our model is its equivalence with a system of two bidimensional harmonic oscillators, the closest particle being repelled by the origin while the farthest is attracted to it. After some time the distances will coincide ("collision") and the role of the two particles are exchanged: thus, the model also belongs to the class of piecewise integrable Hamiltonian systems, among which billiards (see, e.g., ref. 4 and references therein) constitute the best-known example.

2. EQUIVALENCE WITH A SYSTEM OF TWO HARMONIC OSCILLATORS

Let $x_{i\alpha}$ denote the coordinate of particle i $(i=1, 2, 3)$ in direction α $(\alpha=1, 2)$. The area spanned by vertices x_1, x_2, x_3 is

$$\begin{aligned} |K| &= \tfrac{1}{2}\,|\det(x_1-x_3, x_2-x_3)| \\ &= \tfrac{1}{2}\,|(x_{11}-x_{31})(x_{22}-x_{32})-(x_{12}-x_{32})(x_{21}-x_{31})| \end{aligned}$$

Consider the coordinates $(z_1, w_1, g_1, z_2, w_2, g_2)$ related to the previous ones by means of the unitary transformation

$$\begin{pmatrix} z_1 \\ z_2 \\ g_1 \\ w_1 \\ w_2 \\ g_2 \end{pmatrix} = \begin{pmatrix} 0 & \frac{1}{2} & -\frac{1}{2} & \frac{1}{\sqrt{3}} & -\frac{1}{2\sqrt{3}} & -\frac{1}{2\sqrt{3}} \\ 0 & \frac{1}{2} & -\frac{1}{2} & -\frac{1}{\sqrt{3}} & \frac{1}{2\sqrt{3}} & \frac{1}{2\sqrt{3}} \\ \frac{1}{\sqrt{3}} & \frac{1}{\sqrt{3}} & \frac{1}{\sqrt{3}} & 0 & 0 & 0 \\ -\frac{1}{\sqrt{3}} & \frac{1}{2\sqrt{3}} & \frac{1}{2\sqrt{3}} & 0 & \frac{1}{2} & -\frac{1}{2} \\ \frac{1}{\sqrt{3}} & -\frac{1}{2\sqrt{3}} & -\frac{1}{2\sqrt{3}} & 0 & \frac{1}{2} & -\frac{1}{2} \\ 0 & 0 & 0 & \frac{1}{\sqrt{3}} & \frac{1}{\sqrt{3}} & \frac{1}{\sqrt{3}} \end{pmatrix} \begin{pmatrix} x_{11} \\ x_{21} \\ x_{31} \\ x_{12} \\ x_{22} \\ x_{32} \end{pmatrix} \tag{1}$$

(Incidentally, similar transformations occur in the topic referred to as "statistical analysis of shape."[5]) The area spanned by vertices x_1, x_2, x_3 is

$$|K| = \frac{\sqrt{3}}{4} |z_1^2 + z_2^2 - w_1^2 - w_2^2| \tag{2}$$

Kinetic energy transforms as

$$\frac{m}{2} \sum_{i=1}^{3} \sum_{\alpha=1}^{2} \dot{x}_{i\alpha}^2 = \frac{m}{2} (\dot{z}_1^2 + \dot{z}_2^2 + \dot{w}_1^2 + \dot{w}_2^2 + \dot{g}_1^2 + \dot{g}_2^2) \tag{3}$$

Choosing a reference frame where the gravity center is at rest, defining (z, ϕ_z) [resp. (w, ϕ_w)] as the polar coordinates for (z_1, z_2) [resp. (w_1, w_2)], and taking individual rotational invariance into account, we obtain for the energy of the system

$$E = \frac{\kappa}{2} |z^2 - w^2| + \frac{m}{2} \dot{z}^2 + \frac{B_z^2}{2mz^2} + \frac{m}{2} \dot{w}^2 + \frac{B_w^2}{2mw^2} \tag{4}$$

where $B_z := mz^2 \dot{\phi}_z$ and $B_w := mw^2 \dot{\phi}_w$ are the conserved angular momenta, and $\kappa = (\sqrt{3}/2) P$.

As announced, system (4) describes two bidimensional harmonic oscillators of same mass m, *the particle farthest to the origin being attracted to it with coupling constant* κ, *while the particle closest to the origin is repelled by it with coupling constant* $-\kappa$. After some time the distances z and w will coincide ("collision") and the roles of the two particles are exchanged.

Suppose particles collide at time $t = 0$: $z(0) = w(0) = R_0 > 0$, with $\dot{z}(0) > \dot{w}(0)$: the z particle then undergoes harmonic motion,

$$z^2(t) = z^2(0) \cos^2 \omega t + \frac{2z(0)\, \dot{z}(0)}{\omega} \cos \omega t \sin \omega t + \left[\dot{z}^2(0) + \frac{B_z^2}{m^2 z^2(0)} \right] \frac{\sin^2 \omega t}{\omega^2} \tag{5}$$

whereas the w particle undergoes hyperbolic motion:

$$w^2(t) = w^2(0) \cosh^2 \omega t + \frac{2w(0)\, \dot{w}(0)}{\omega} \cosh \omega t \sinh \omega t + \left[\dot{w}^2(0) + \frac{B_w^2}{m^2 w^2(0)} \right] \frac{\sinh^2 \omega t}{\omega^2} \tag{6}$$

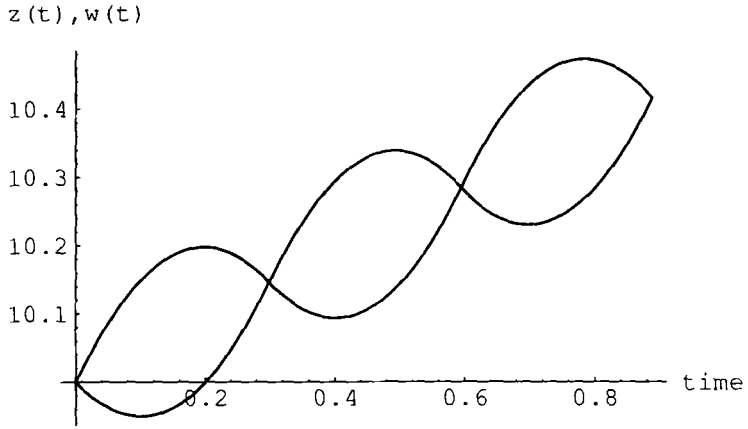

Fig. 1. The b-trajectory ($t \in [0, t_3]$).

with $\omega^2 = \kappa/m$. In the sequel, $z(t)$ and $w(t)$ will denote distances to the origin of respectively the "harmonic" particle and the "hyperbolic" one $[z(t) \geqslant w(t)]$. Collision times are $t_k = \sum_{j=1}^{k} \tau_k$ [τ_k is the time between the $(k-1)$th and kth collisions] and the collision distances satisfy $R_k := z(t_k) = w(t_k)$.

Velocities and angular momenta get exchanged at collisions: $\dot{z}_k := \dot{z}(t_k^+) = \dot{w}(t_k^-)$, $B_z(t_k^+) = B_w(t_k^-)$, $\dot{w}_k := \dot{w}(t_k^+) = \dot{z}(t_k^-)$, $B_w(t_k^+) = B_z(t_k^-)$. Figure 1 shows the three first collisions undergone by a typical trajectory, and Fig. 2 depicts the corresponding phase space portrait: those colli-

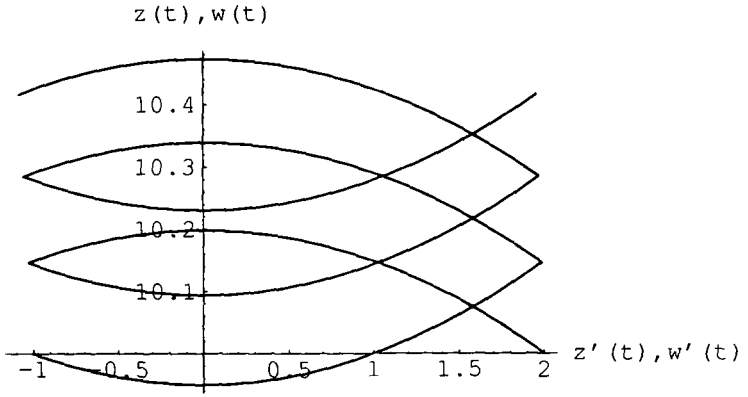

Fig. 2. Phase portrait for the b-trajectory ($t \in [0, t_3]$).

sions [corresponding in the initial system to the vanishing of $|K| = \frac{1}{2}|\det(x_1 - x_3, x_2 - x_3)|$, i.e., to orientational breaking] leave little hope of achieving analytical mastery. Further investigations have been carried out using adiabatic limits, supported by numerical simulations in combination with discrete recurrence relations and fixed-point convergence arguments.

3. NUMERICAL SIMULATIONS

A series of empirical simulations with various initial conditions show two types of trajectories:

(a) Trajectories apparently escaping to infinity: $R_k \to \infty$ when $k \to \infty$, with $\tau_k \to 0$. Figures 3–5 show, respectively, the positions $z(t)$, $w(t)$ for $n = 30$ collisions (all happens as if one were dealing with a *single free particle*: z and w are barely individually distinguishable at this scale), the collision times τ_k versus k ($n = 400$), and a Poincaré section $(\dot{z}_k, z_k)$ for the a-trajectory with initial conditions $m = k = 1$, $B_z^2 = B_w^2 = 4$, $z(0) = w(0) = 10$, $\dot{z}(0) = 2$, and $\dot{w}(0) = 1$.

(b) Trajectories quasiperiodically confined near the origin; τ_k strongly increases as R_k approaches its minimum. Figures 6 ($n = 100$), 7, and 8 ($n = 400$) correspond to Figs. 3–5 for the b-trajectory with initial conditions $m = k = 1$, $B_z^2 = B_w^2 = 4$, $z(0) = w(0) = 10$, $\dot{z}(0) = 2$, and $\dot{w}(0) = -1$: both kinetic and potential initial energies are the same for a- and b-trajectories, differing only by the sign of $\dot{w}(0)$. The b-trajectory is characterized by a

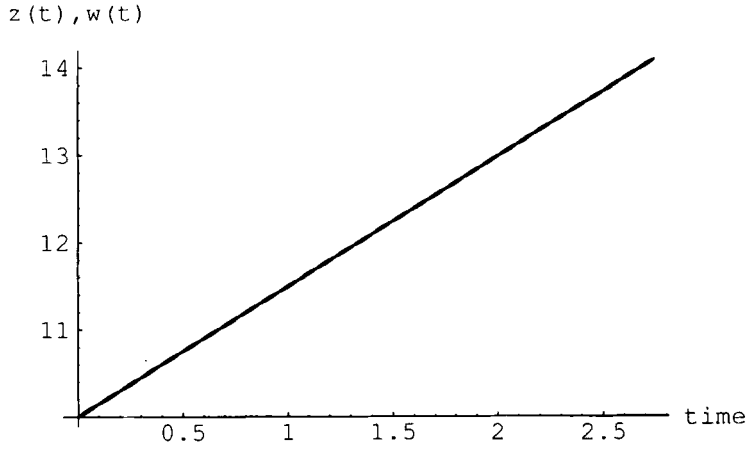

Fig. 3. The a-trajectory ($t \in [0, t_{30}]$).

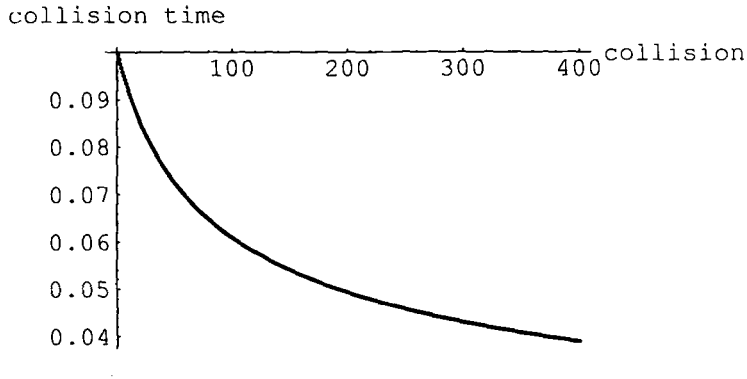

Fig. 4. $\tau(k)$ for the a-trajectory ($k \in [0, 400]$).

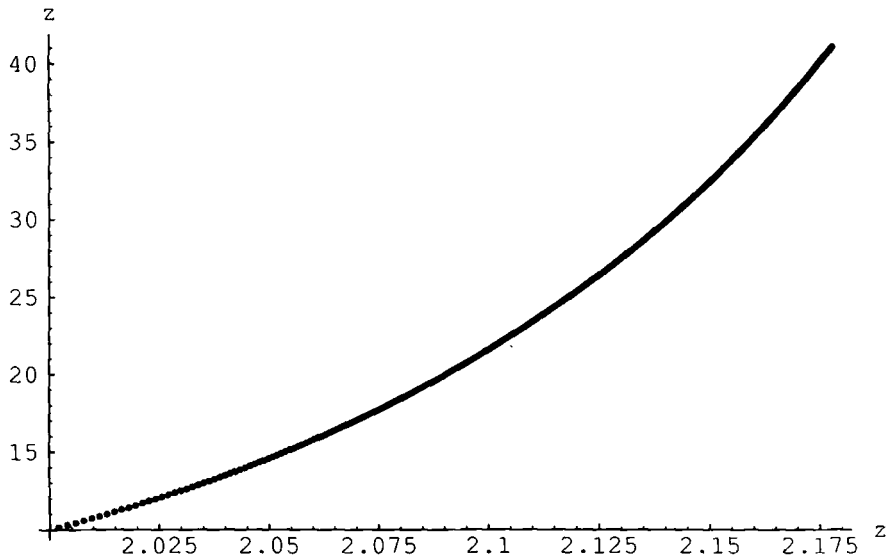

Fig. 5. Poincaré section for the a-trajectory ($k \in [0, 400]$).

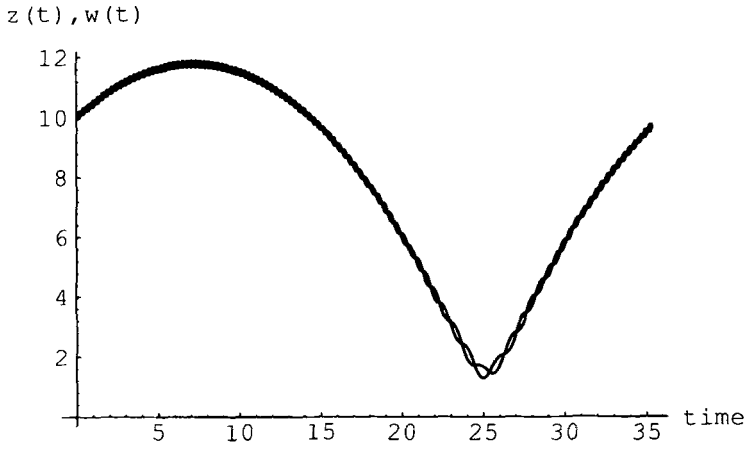

Fig. 6. The b-trajectory ($t \in [0, t_{100}]$).

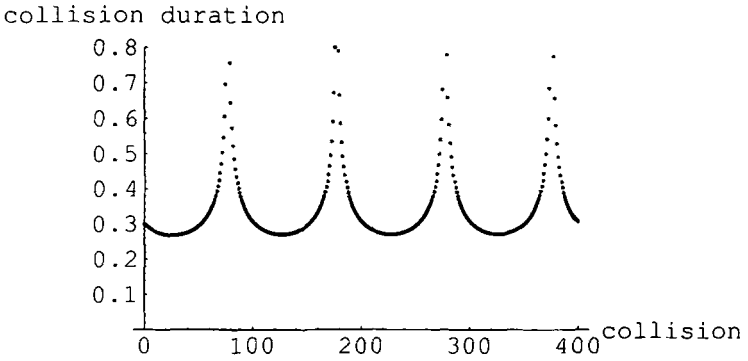

Fig. 7. $\tau(k)$ for the b-trajectory ($k \in [0, 400]$).

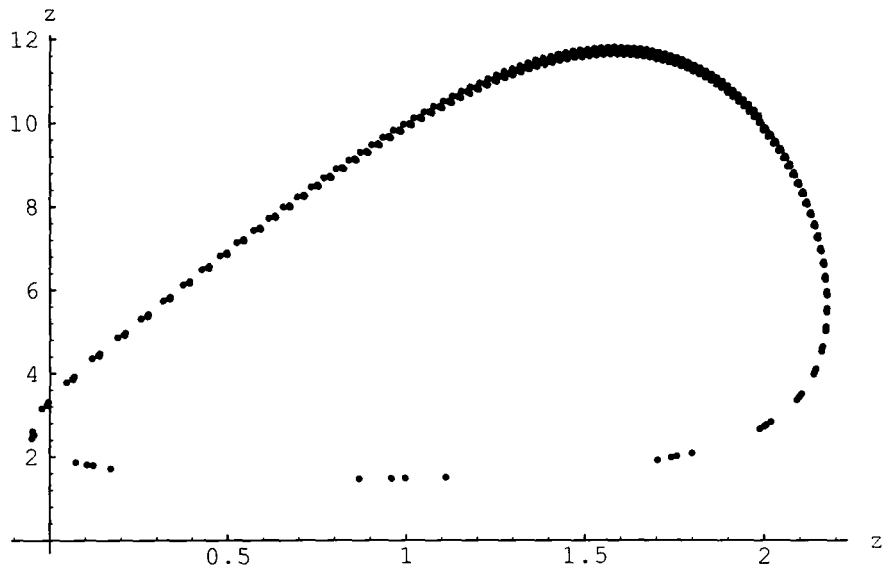

Fig. 8. Poincaré section for the b-trajectory ($k \in [0, 400]$).

quick motion of period of order $\tau \simeq 0.3$ (collisions) and a slow one of period $T \simeq 100$ (quasiperiodic "precession").[2]

4. ADIABATIC LIMIT (I)

The latter is most coveniently carried over in coordinates $u := (1/\sqrt{2})(z+w)$ and $v := (1/\sqrt{2})(z-w)$. The energy (4) reads

$$E = \kappa\,|uv| + \frac{m}{2}\dot{u}^2 + \frac{m}{2}\dot{v}^2 + \frac{B_z^2}{m(u+v)^2} + \frac{B_w^2}{m(u-v)^2} \tag{7}$$

The symmetry $u \leftrightarrow v$ is broken by the constraint $u \geqslant v \geqslant 0$ reflecting $z \geqslant w \geqslant 0$. Collisions correspond to specular reflections on the line $v = 0$, whereas the line $u = v$ can be shown to correspond to isoceles configurations of the original triangle. Figure 9 depicts the a-trajectory ($n = 30$) in the u–v plane.

[2] Confinement of the trajectory implies $\langle \dot{z}(t) \rangle = 0$ *on average*, as illustrated in Fig. 6. However, $\dot{z}(t_k) > 0$ for (most of) the *collision times*, as illustrated in Fig. 8. I thank a referee for pointing out this difficulty.

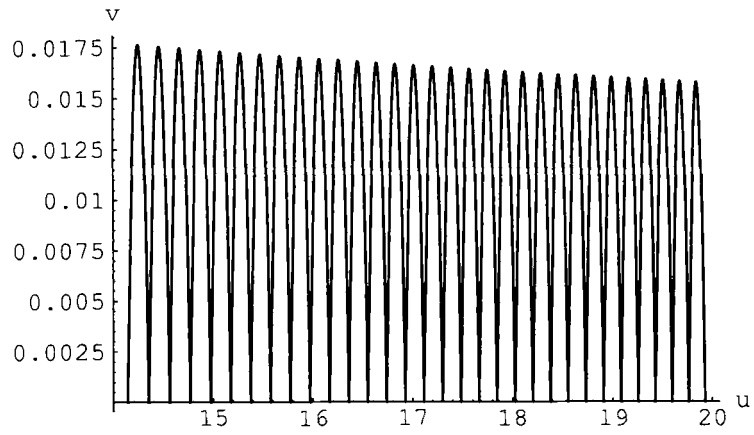

Fig. 9. The a-trajectory ($t \in [0, t_{30}]$).

The u coordinate (overall distance to origin) describes slow motion: the v coordinate (relative distance) describes the rapid one, governed by effective energy

$$E_{\text{eff}} = \kappa u\,|v| + \frac{m}{2}\dot{v}^2 = \frac{m}{2}\dot{v}^2(0^+)$$

where $\dot{v}(0^+) > 0$, the velocity just after some collision we take as the temporal origin, is adiabatically invariant.

By energy conservation, the period τ between two collisions is[6]

$$\tau = \frac{2\dot{v}(0^+)}{\omega^2 u(0)} = \frac{\dot{z}(0^+) - \dot{w}(0^+)}{\omega^2 z(0)} \tag{8}$$

The average potential acting on u is

$$-\kappa u \langle v \rangle_\tau = \frac{2}{3} E_{\text{eff}} = \frac{m}{3}\dot{v}^2(0^+)$$

(by the virial theorem): this suggest the possibility for the u coordinate to become asymptotically free, approaching a constant velocity $\dot{u}_\infty$.

However, the velocity of a slow particle varies for finite distances as

$$\Delta\dot{u} := \dot{u}(\tau) - \dot{u}(0) = -\frac{\kappa}{m}\int_0^\tau v(t)\,dt \simeq -\frac{\tau}{mu_0}\langle \kappa v u \rangle_\tau$$

With (8) and the virial theorem again

$$\Delta\dot{u} = -\frac{2\dot{v}^3(0^+)}{3\omega^2 u^2(0)} \tag{9}$$

Let u_k denote the u coordinate at the kth collision, and $\dot{u}_k$ its velocity. Together with (8) and (9), we get the system

$$\begin{cases} u_{k+1} = u_k + a\dfrac{\dot{u}_k}{u_k} \\ \dot{u}_{k+1} = \dot{u}_k - \dfrac{b}{u_k^2} \end{cases} \quad \text{where} \quad \begin{cases} a = \dfrac{2\dot{v}(0^+)}{\omega^2} > 0 \\ b = \dfrac{2\dot{v}^3(0^+)}{3\omega^2} > 0 \end{cases} \tag{10}$$

or equivalently, the second-order evolution

$$u_{k+2} = u_{k+1} + u_k - \frac{1}{u_{k+1}}\left(\frac{ab}{u_k^2} + \dot{u}_k^2\right) \tag{11}$$

Recall that (11) holds in the adiabatic limit only, where $u_k > 0$ is large enough and the centrifugal barrier B_-, B_+ negligible. In this limit, we prove that *u-motion is always bounded, i.e., contrarily to what Figs.* 1–3 *suggest, the system always returns near the origin.* In short, escaping trajectories would be *metastable*: their perceived stability might be convincing for (very) long but finite times, smaller than the precession time T (we have observed the a-trajectory during $k_{\max} = 10000$ collisions without any noticeable qualitative change).

Proof. Consider $e_k := (2b/a)\ln u_k + \dot{u}_k^2$. Existence of an asymptotically free u motion ($u_\infty = \infty$, $\dot{u}_\infty \geqslant 0$) makes $e_\infty = \infty$. On the other hand,

$$e_{k+1} = e_k + \frac{b}{u_k^4}(b - a\dot{u}_k^2) + O(u_k^{-6}) \tag{12}$$

Divergence of e_k entails $\lim_{k\to\infty}(b - a\dot{u}_k^2) \geqslant 0$ and u_k growing at most as $ck^{1/4}$. Then (10) yields the contradiction $\dot{u}_\infty = \dot{u}_0 - b\sum_{k=0}^{\infty}(1/u^2 k) = -\infty$. ∎

In physical terms, e_k mimics an energy whose logarithmic potential $(2b/a)\ln u_k$ insensitively but inexorably imprisons the particle u_k.

5. ADIABATIC LIMIT (II)

Comparison with simulations shows approximations (8) and (9) to hold well; what is more worrying is the drift of $\dot{v}(t_k^+)$ (Fig. 10, a-trajectory) due to nonconstancy of u between collisions. Let $v(0^+) = 0$, $\dot{v}(0^+) > 0$, be

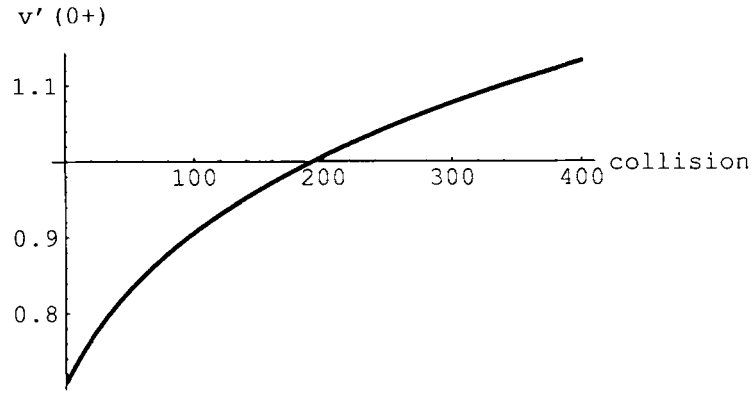

Fig. 10. Relative velocity after collisions (a-trajectory).

given. The particle is then reflected at time s such that $\dot{v}(s) = [\int_0^s dt\, \ddot{v}(t)] + \dot{v}(0^+) = 0$, i.e., such that $\dot{v}(0^+) = \omega^2 \int_0^s dt\, u(t)$. Then the particle returns to the origin at time $s + s'$ such that $v(s + s') = 0$. Its velocity just before collision is

$$\dot{v}((s+s')^-) = \left[\int_0^{s'} dt\, \ddot{v}(s+t)\right] + \dot{v}(s) = -\omega^2 \int_0^{s'} dt\, u(s+t)$$

Then

$$\Delta\dot{v} := \dot{v}(\tau^+) - \dot{v}(0^+) = \omega^2 \left[\int_0^{s'} dt\, u(s+t) - \int_0^s dt\, u(t)\right]$$

Taking $u(t) \simeq u(0) + t\dot{u}(0)$, and $s \simeq s' \simeq \tau/2$, one finally gets

$$\Delta\dot{v} = \frac{\dot{u}(0)\, \dot{v}^2(0^+)}{\omega^2 u^2(0)} \tag{13}$$

System (10) should then be replaced by

$$\begin{cases} u_{k+1} = u_k + \dfrac{2\dot{u}_k \dot{v}_k}{\omega^2 u_k} \\ \dot{u}_{k+1} = \dot{u}_k - \dfrac{2\dot{v}_k^3}{3\omega^2 u_k^2} \\ \dot{v}_{k+1} = \dot{v}_k + \dfrac{\dot{u}_k \dot{v}_k^2}{\omega^2 u_k^2} \end{cases} \quad \text{or} \quad \begin{cases} u_{k+1} = u_k + \dot{u}_k \tau_k \\ \dot{u}_{k+1} = \dot{u}_k - \dfrac{\omega^4}{12} u_k \tau_k^3 \\ \tau_{k+1} = \tau_k - \dfrac{\dot{u}_k \tau_k^2}{2u_k} \end{cases} \tag{14}$$

Only first-order terms have been retained: the adiabatic approximation is valid for $u_k \gg \tau_k \dot{u}_k$, $u_k \gg \tau_k \dot{v}_k$. Defining $\alpha_k := \dot{u}_k / u_k$, one gets with the same approximation

$$\begin{cases} u_{k+1} = u_k + u_k \alpha_k \tau_k \\ \alpha_{k+1} = \alpha_k - \left(\dfrac{\omega^4}{12} \tau_k^3 + \alpha_k^2 \tau_k \right) \\ \tau_{k+1} = \tau_k - \dfrac{1}{2} \alpha_k \tau_k^2 \end{cases} \tag{15}$$

Collision times turn out to satisfy a second-order autonomous recurrence relation:

$$\tau_{k+2} = \tau_{k+1} \left(f\left(\frac{\tau_{k+1}}{\tau_k} \right) + c\tau_k^4 \right) \quad \text{or} \quad \begin{cases} q_{k+1} = f(q_k) + c\tau_k^4 \\ \tau_{k+1} = q_k \tau_k \end{cases} \tag{16}$$

where $q_k := \tau_{k+1}/\tau_k$, $c = \omega^4/24$, and $f(x) := 1 + x - 3x^2 + 2x^3$.

Before discussing the system (16), recall that τ_k is decreasing iff u_k is increasing.

Suppose $c = 0$. Figure 11 then shows the evolution $q_{k+1} = f(q_k)$ with initial condition $q_0 > 0$ to converge to $q_\infty = 1$ [the fixed point $1 = f(1)$ is stable to the left] iff $1/2 < q_0 < 1$: this corresponds to indefinitely escaping trajectories. For $0 \leqslant q_0 \leqslant 1/2$ or $q_0 \geqslant 1$, $q_\infty = \infty$: corresponding trajectories are the reflected ones.

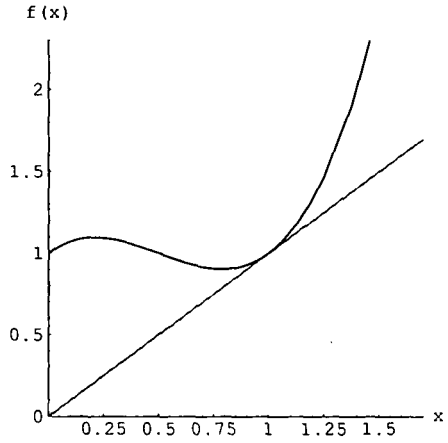

Fig. 11. Left stability of $1 = f(1)$.

For $c>0$, it is convenient to introduce $\varepsilon_k := 1-q_k$, which we take as a small, positive quantity (u_k increasing). From (16)

$$\begin{aligned}\varepsilon_{k+1} &= 1 - f(1-\varepsilon_k) - c\tau_0^4 \prod_{j=0}^{k} (1-\varepsilon_j)^4 \\ &\simeq \varepsilon_k - 3\varepsilon_k^2 - c\tau_0^4 \exp\left(-4\sum_{j=0}^{k}\varepsilon_j\right)\end{aligned} \tag{17}$$

Set $E(k) := \sum_{j=0}^{k} \varepsilon_j$ and $C := c\tau_0^4$. In the continuum limit, (17) amounts to

$$E''(k) \cong -3[E'(k)]^2 - C\exp[-4E(k)] \qquad \text{with} \quad E(0)=0 \text{ and } E'(0)=\varepsilon_0 \tag{18}$$

$E(k)$ is increasing as long as $\varepsilon_k \geqslant 0$. As soon as $\varepsilon_k \leqslant 0$, the trajectory is reflected. Define $x(k) := \exp[3E(k)]$. Then $x''(k) = -3C/x^{1/3}(k)$ describes the motion of a particle of unit mass in potential $V(x) = (9/2)\,Cx^{2/3}$ with initial conditions $x(0)=1$, $x'(0)=3\varepsilon_0$. The particle gets reflected at collision k_1 satisfying $x'(k_1)=0$, i.e.,

$$\begin{aligned}k_1 &= \frac{1}{3}\int_1^{(\varepsilon_0^2/C+1)^{3/2}} \frac{dx}{(\varepsilon_0^2 + C - Cx^{2/3})^{1/2}} \\ &= \frac{1}{2C^{3/2}}\left[(\varepsilon_0^2+C)\left\{\frac{\pi}{2} - \arctan\frac{\sqrt{C}}{\varepsilon_0}\right\} + \varepsilon_0\sqrt{C}\right]\end{aligned} \tag{19}$$

Define $s_0(k)$ as the number of collisions (measured from the start of simulation) occurring between collision k and the u reflection towards the origin. By construction, $s_0(0) =: k_0$ is the duration of increasing u_k behavior and $s_0(k)$ should logically be of the form $s_0(k) := k_0 - k$ for $k \leqslant k_0$, periodically extended as $s_0(k) = T - ((k-k_0) \bmod T)$, where T is the precession period. On the other hand, formula (19) worked out in terms of (τ_k, τ_{k+1}) instead of (τ_0, τ_1) yields

$$\begin{aligned}s_1(k \mid \tau_1, \tau_2) = &\left[\frac{24\sqrt{6}}{\omega^3\tau_k^5}(\tau_{k+1}-\tau_k)^2 + \frac{\sqrt{6}}{\omega^2\tau_k^2}\right]\left[\frac{\pi}{2} - \arctan\frac{\omega^2\tau_k^3}{2\sqrt{6}(\tau_k - \tau_{k+1})}\right] \\ &+ \frac{12(\tau_k - \tau_{k+1})}{\omega^4\tau_k^5}\end{aligned} \tag{20}$$

Note $\lim_{\omega \to 0} s_1(k) = \infty$: this matches the stability of the fixed point $q_\infty = 1^-$ for $c=0$. Moreover,

$$\lim_{(\tau_{k+1} \to \tau_k^-)} s_1(k) = 0 \qquad \text{and} \qquad \lim_{(\tau_{k+1} \to \tau_k^+)} s_1(k) = \frac{\pi\sqrt{6}}{\omega^2\tau_{\min}^2}$$

Figure 12 shows the graph of $s_1(k)$ obtained from simulated values (τ_k, τ_{k+1}) of the b-trajectory compared to the graph of $s_0(k)$ where $T \simeq 102 =$ period of u motion, $k_0 \simeq k_1 \simeq 26$ $(u_{k_0} = u_{\max})$: the agreement of $s_0(k)$ and $s_1(k)$ is pretty good except in a neighborhood of $\tilde{k} := k_0 + T/2 \simeq 77$, where the particle is too close to the origin $(u_{\tilde{k}} = u_{\min})$ for the adiabatic approximation to remain valid. Although (20) was derived under the hypothesis of increasing u_k, it obviously holds well in decreasing conditions also (time reversibility): given any two consecutive short periods, *formula* (20) *correctly estimates the waiting time till the next u reflection, provided measurement is performed not too close to the origin.*

Moreover, estimating the discontinuity of $s_0(k)$ at $k = k_0$ by the corresponding jump of $s_1(k)$ yields the following relationship between short (collisions) and long (precession) periods:

$$T = \frac{\pi\sqrt{6}}{\omega^2 \tau_{\min}^2} \tag{21}$$

Figure 7 yields $\tau_{\min} = \tau_{k_0} = 0.269$, whereas formula (21) with $T = 102$ yields $\tilde{\tau}_{\min} = \tau_{k_0} = 0.275$. Observation of other trajectories confirms the genericity of the relation.

Also, although taking into account $\Delta\dot{v}$ constitutes an improvement over description of Δu and $\Delta\dot{u}$ only, qualitative predictions are quite similar in both models: In particular, the analog of (16) can be derived from (10), yielding $q_{k+1} = \tilde{f}(q_k) + \tilde{c}\tau_k^4$, where $\tilde{f}(x) = 1 - x^2 + x^3$ and $\tilde{c} = \omega^4/12$; u reflection then reduces to x reflection $[x := \exp 2E(k)]$ in potential $\tilde{V}(x) = 2\tilde{C} \ln x$: so it is not unreasonable to image our method of predicting return time as well as short/long-period relation of type (21) to be of some generality.

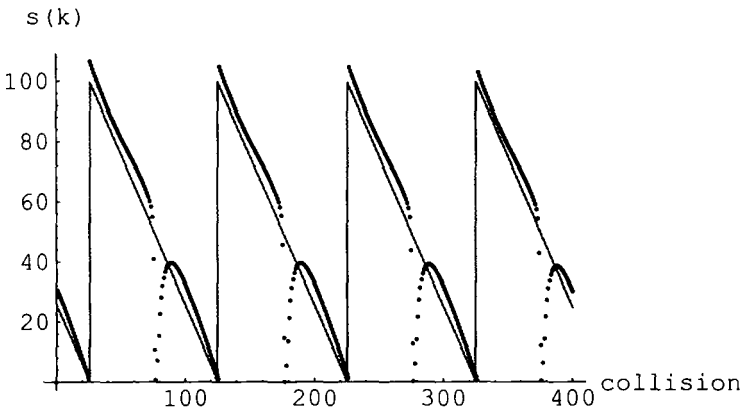

Fig. 12. Theoretical versus empirical lifetime of escaping behavior.

6. CONCLUSIONS

One thing is certain: our model is not ergodic; for if it were, the proportion of time spent around u (integrating over v, $\dot{u}$, $\dot{v}$ at fixed energy: microcanonical measure) would go as u^{-1}. Nonnormalizability of the latter (i.e., logarithmic divergence of the partition function) ruins ergodicity; this is compatible with both the following mutually exclusive and exhaustive statements:

- A: The a-trajectory and related ones vanish at infinity: z and w particles become bound to each other by an infinite force and can no longer be individually discerned [$\tau_\infty = 0$, $(v_{\max})_\infty = 0$]: to this confinement corresponds an increasingly stretched (obtuse) triangle in the original (x_1, x_2, x_3) coordinates. The large side (diameter) moves with velocity $\sqrt{2}\dot{u}_\infty$, while the corresponding height oscillates at frequency $\omega_v = 2\pi/\tau \to \infty$. Divergence of partition function supports this picture.[1]
- B: The a-trajectory and related ones are always reflected due to nonergodic confinement mechanisms. Triangular dynamics consists of quasiperiodic precession of its diameter between $D_{\min}$ and $D_{\max}$, modulated by rapid orientational inversions: here, a-type triangles do not evaporate, even if their very persistent tendency to dilution can be qualified as metastable.

Another reliable fact is the inability of adiabatic theories to take into account behavior A, if existing. As the latter stems from averaging rapid processes, and so stands, so to speak, halfway between mechanics and statistical mechanics, one is tempted to put more credit in adiabatic theory than statistical mechanics when their descriptions are conflicting. That is, rejection of A from adiabatic arguments appears stronger than its acceptance on a statistical mechanical basis.

The a-trajectory, if confined, presumably obeys relation (20), yielding $s_1(0) \simeq 9500$ as initial estimate of escaping behavior duration. At 10,000 collisions later, the estimate has grown to $s_1(10{,}000) \simeq 33{,}000$: this does not contradict the qualitative behavior of $s_1(k)$ depicted in Fig. 12 provided observations take place "just after" maximal proximity to the origin. In this regime, $s_1(k) < s_0(k)$ and so T would be at least 66,000.

The original system (4) or (7) contains four degrees of freedom with one integral of motion (the energy). Adiabatic limits I and II contain, respectively, two and three degrees of freedom without obvious conserved quantity: dimensionally speaking, theory II then might (or might not) capture the true nature of the motion. Of course, nothing forbids in theory the existence of another integral of motion for the original system, a suspicion partially supported by the contrast between a- and b-behavior

despite the identity in energy. However, nonergodicity is far from implying integrability, as illustrated by KAM theorem.

Finally, the quantum analog of the area model has *pure discrete spectrum*, as noted by Simon,[3] as a consequence of the Fefferman–Phong theorem. Also, the quantum partition function is finite. So behavior A, if existing, possesses no quantum analog.

ACKNOWLEDGMENTS

It is a great pleasure to dedicate this paper to Prof. Philippe Choquard, my former thesis advisor, to whom I am gratefully indebted for his knowledge, attention, and generous encouragement. Preparation of this paper reminded me of happy times in the context of his lectures in mécanique analytique at the EPF-Lausanne.

REFERENCES

1. F. Bavaud, Statistical mechanics of convex bodies, *J. Stat. Phys.* **57**:1059–1068 (1989); F. Bavaud, Isoperimetric phase transitions of two-dimensional droplets, *Commun. Math. Phys.* **132**:549–554 (1990).
2. A. Carnegie and I. C. Percival, Regular and chaotic motion in some quartic potentials, *J. Phys. A* **17**:801–813 (1984).
3. B. Simon, The classical limit of quantum partition function, *Commun. Math. Phys.* **71**:247–276 (1980); B. Simon, Some quantum operators with discrete spectrum but classically continuous spectrum, *Ann. Phys. (N.Y.)* **146**:209–220 (1983).
4. T. Dagaeff and C. Rouvinez, On the discontinuities of the boundary in billiards, *Physica D* **67**:166–187 (1993).
5. D. G. Kendall, Exact distributions for shapes of random triangles in convex sets, *Adv. Appl. Prob.* **17**:308–329 (1985); C. R. Goodall and K. V. Mardia, Multivariate aspects of shape theory, *Ann. Stat.* **21**:848–866 (1993).
6. L. Landau and E. Lifchitz, *Mécanique* (Mir, Moscow, 1969).